Energy Conversion and Management 269 (2022) 116169

Contents lists available at ScienceDirect

Energy Conversion and Management

journal homepage: www.elsevier.com/locate/enconman

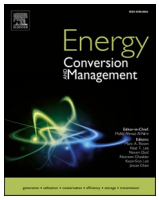

Assessment of the differential impact of scroll and sliding vane rotary expander permeability on the energy performance of a small-scale solar-ORC unit

Fabio Fatigati *, Diego Vittorini, Arianna Coletta, Roberto Cipollone

University of L'Aquila, Department of Industrial and Information Engineering and Economics, Piazzale Ernesto Pontieri, Monteluco di Roio, 67100 L'Aquila, Italy

ARTICLE INFO

Keywords:
Solar driven Organic Rankine Cycle
Scroll Expander
Sliding rotary vane expander
Cogeneration
ORC control

ABSTRACT

Organic Rankine Cycle ORC-based power unit is a suitable solution for combined heat and power (CHP) generation in the residential sector currently responsible for an average 28 % energy-related CO_2 emissions. The ability to tolerate seasonal daily and hourly fluctuations of the available thermal energy without significant performance compromission – i.e. efficiency of electricity generation and domestic hot water (DHW) fulfillment – is crucial. The need for the plant to work under severe off-design conditions affects the expander selection which for such plants are generally of volumetric technology. The most up-to-date literature addresses scroll-type and sliding vane rotary (SVRE) expanders as the most effective options. For such reason the present paper deals with the experimental assessment of the energy performance of an ORC-based plant equipped with both a custom-design SVRE and a scroll expander. The ORC unit assumes the same plant configuration in the two cases except for the expander layout. SVRE is connected through a mechanical joint to the electric generator whereas the scroll expander shares the same shaft and casing with the electric machine. The former approach ensures to control the expander speed which is set by the dynamic equilibrium in the latter case. The comparative analysis provides useful insights on the relative advantage of both technologies and configuration and a clear indication on the different operating strategy required in each case. SVRE leads to an electric output of the power unit in the 200–700 W range with a 2–6% efficiency whilst scroll expander is associated with a 100–500 W power range and a 2–4% efficiency partly compensated with a shorter starting time and a larger operability range (17–60 g/s). Despite SVRE is regulated in revolution speed its efficiency (20–40 %) is lower than the scroll one (40–60 %). The experimental assessment of the power unit was coupled with an in-depth modeling activity to address the impact of the expander operating conditions mainly on the inlet expander pressure which is close to the upper pressure of the thermodynamic cycle. The model derived from a theoretical analysis of the expander permeability focuses on the effect of the expander revolution speed – variable in the SVRE case constrained in the scroll case – and provides good accuracy with a Root Mean Square Error below 4 % in both cases.

1. Introduction

In recent years solar thermal technologies have become increasingly interesting due to their growing cost-competitiveness [1] and their technological improvements in terms of efficiency [2]. These systems use a heat transfer fluid to convert solar radiation into thermal energy which can be exploited either directly for heating purposes or converted into mechanical work via a power cycle [3]. The Organic Rankine cycle (ORC) technology is the most viable option [4] due among other characteristics to the high compatibility between the operating temperatures of solar thermal technologies and the temperature needs of the cycle [5]. Particularly small-scale ORC units are characterized by good characteristic efficiencies adaptability to several temperature ranges and ease of use and maintenance [6]. The main issues of solar-based ORC plants are in the low energy density of the solar source and its intermittent nature preventing the continuous operation of the plant and the generation of a cost-justifying energy output. Nonetheless to the scopes of the solar-ORC plant both problems can be mitigated by integrating a thermal storage unit into the system [3].

Solar-based ORC plants are often used for simultaneous heat and power (CHP) generation with higher efficiency lower economic cost and reduced emissions than separate production [7,8]. Several studies have also proposed the integration of solar-ORC plants with poly-generation

* Corresponding author.
E-mail address: fabio.fatigati@univaq.it (F. Fatigati).

https://doi.org/10.1016/j.enconman.2022.116169
Received 7 June 2022; Received in revised form 28 July 2022; Accepted 18 August 2022
Available online 31 August 2022

Nomenclature

Symbols

k'	revolution speed regression line slope [rps/ kg/s]
k''	volumetric efficiency regression line slope [kg/s]$^{-1}$
$\dot{m}$	working fluid mass flow rate [kg/s]-[g/s]
Q_1	Hot source thermal power [kW]
q'	revolution speed regression line y-intercept [rps]
q''	volumetric efficiency regression line y-intercept
P	Power [W]
R	Specific gas constant [J/kgK]
T	Temperature [K]
V	Volume [m^3]
Z	compressibility factor
1	Condenser inlet
2	Condenser outlet/pump inlet
3	Pump outlet/evaporator inlet
4	Evaporator outlet/expander inlet
5	Expander output

Subscript

ad,is	adiabatic isentropic condition
in	inelt/intake
out	outlet
exp	expander
hw	hot water
pump	volumetric pump
sat	saturation
th	theoretical
vol	volumetric
wf	working fluid

Greek Symbols

α	permeability [kg/(Pas)]
Δ_p	pressure rise [bar]-[Pa]
η	efficiency
ω	revolution speed [rpm]-[rps]
ρ	density [kg/m^3]

Acronyms

CW	Cold Water
HW	Hot water
ORC	Organic Rankine Cycle
PHRVG	Plate Heat recovery Vapor generator
PHX	Plate Heat Exchanger
SH	Super heated
SVRE	Sliding Rotary Vane Expander
WF	Working fluid

units [9] which allow to obtain multiple energy outputs such as tri-generation [10–12] and desalination [13]. In [10] a Solar ORC cascade refrigeration system is developed achieving a thermal efficiency and exergy efficiency respectively equal to 89.4 % and 8.70 %. The trigeneration system presented in [11] is based on parabolic trough solar collector and thermal energy storage tank and ensures to achieve energy and exergy efficiency respectively equal to 34.8 % and 13.4 %. In [12] a novel heating cooling and power system based on a proper combination of ORC Ejector Refrigeration Cycle (ERC) and Domestic Hot Water Heater (DWH) is proposed achieving an energy efficiency equal to 34.14 %. In [13] a combination of photovoltaic-thermal Mechanical Vapor Compression desalination and ORC systems is presented for freshwater and electricity production for the domestic sector. Considering a solar radiation of 500 W/m^2 the whole system produces 141 m^3/d of distilled water produced and 37.8 kW of net power with an electrical efficiency of almost 7.6 %.

Thanks to their compact sizing [6] solar-based ORC plants are the most suitable solution to be used in residential CHP for producing power and domestic hot water (DHW). These systems can play a significant role in reducing emissions from buildings which were responsible for 28 % of global energy-related CO_2 emissions in 2019 [14]. Plenty of studies have investigated the performance of solar-powered ORC plants with particular attention to the effects of (i) operation parameters and (ii) the working fluid type which affects the system efficiency the components size the design of expansion machine and the economic performance [15]. Piñerez et al. [2] evaluated the effect on solar-ORC performance of three different organic fluids (toluene cyclohexane and acetone) using radiation data from four locations and performed an exergetic analysis to evaluate the behavior of each system component as the working fluid changes. Mosaffa et al. [12] proposed a system for simultaneous power heating and cooling production and presented an energetic exergetic and economic analysis for four different organic fluids (R123 R236fa R245fa R600a). Marinheiro et al. [16] analyzed the transient performance of the power plant using solar radiation data from three different locations for three working fluids (R1233zd (E) R600a R245fa). Hu et al. [17] analyzed the effect of the type of working fluid the generation temperature the condensation and the evaporation temperature on the performance of the system. Yu et al. [18] evaluated the performance of the system according to the configuration (with or without recuperator) the working fluid and the operating modes (subcritical or supercritical).

Despite several works on ORC systems bottoming concentrating solar collectors [8] non-concentrating technologies are currently receiving great attention [6,19,20]. Concentrating collectors allow to reach higher temperatures and higher thermodynamic efficiencies in the ORC unit [5] but the plant costs are higher [21] and the use of tracking devices and efficient storage of thermal energy seriously question the feasibility of small-scale units [5]. Moreover via appropriate selection of the heat transfer fluid working fluid and rotary machines it is possible to improve the performance of the ORC plant served by non-concentrating collectors thus filling the performance gap with ORC units with concentrating devices [21]. For small scale power plants volumetric expanders are commonly preferred to dynamic machines due to their higher suitability to unsteady operating conditions [22] and low cost high reliability and suitability with low operational speed [21] capability to deal with dual phase expansions. The selection of the expander type and the cycle operating pressures are mutually constrained and they both affect the cycle efficiency and the power output of the unit [23–25]. As a matter of fact the maximum pressure of the cycle depends on the permeability of the machine which is analytically defined as the ratio between the inlet flow rate to the expander and the difference between the inlet and outlet pressure (the latter can be considered constant because it is fixed by the conditions of the cold source). Therefore for a fixed flow rate of working fluid the lower the permeability of the machine the higher the expansion ratio on which the power produced by the system depends; vice versa the higher the permeability the lower the expansion ratio. Moreover expander permeability defines a linear relation between plant maximum pressure and mass flow rate [24] for a SVRE operating at fixed speed. This means that these two parameters cannot be independently considered but operating paths exist. This dependence was theoretically investigated by varying the SVRE's speed [24] whose immediate result is an expander permeability change. Despite this importance it is noteworthy to observe that the permeability concept is relatively novel in literature and to the best authors knowledge it is not enough referenced for the expander selection nor for its control particularly for micro-cogeneration recovery units. This concept assumes a particular importance due the intrinsic variability of the low-grade heat sources (when

they come from renewable sources for instance). In this case the variation of the mass flow rate of working fluid is the first and easiest control parameter. The management of the off design also needs to readjust the mass flow rate circulating inside the recovery unit. So due to the relation between flow rate and maximum pressure suitable control actions of the expander (i.e. of the recovery unit) can make profit from this relationship in order to keep the same maximum pressure which defines all the thermodynamic properties of the unit.

This paper considers a small ORC-based recovery unit fed by solar energy stored as hot water inside a proper thank. This to widen the solar energy recovery to the production of electrical energy so realizing a micro-cogeneration system. For this purpose the variation of the working fluid flow rate of the unit has a great importance both to maximize the solar energy recoverable (the discharging of the thermal energy from the reservoir produced by the recovery unit allows a further solar energy recovery) and the cogeneration function. In order to manage the SVRE behavior the speed of rotation of it has been controlled in speed ensuring that the connection to the grid was always compatible (fixed frequency electricity generation). So the permeability of the machine was fully controlled i.e. the maximum plant pressure if required.

Considering that the unit operates with an upper thermal source given by hot water produced by solar flat panels any improvement is particularly advisable also in terms of reliability. Being the expander the most important component in terms of net electricity produced. In this paper a scroll machine has been also considered as expander privileging a hermetic version for safety and simplicity. This machine being of a volumetric type is particularly suitable (as it happens for SVREs) to deal with highly variable operating conditions. Due to the hermetic set up of the machine the speed of revolution can't be controlled but it results from the flow rate which has been used as control parameter of the unit. Also in this case the permeability concept demonstrated very effective allowing to evaluate the maximum operating pressure of the unit. No similar knowledge was found in literature in order to support expander choice control and operability for so small recovery units.

In the present paper the results of the experimental assessment of a solar-based ORC unit featuring either a scroll expander or a sliding rotary vane expander (SVRE) were compared. The relationship between the expander permeability and the power output of the unit were also assessed by varying the amount of thermal energy inside the reservoir according to different boundaries. The two expanders adopt two different control schemes with the SVRE speed controlled and the scroll expander load driven with the speed resulting from the mechanical balance of -the shaft. Thanks to the wide experimental analysis an analytic model of the expander permeability for the two machines was developed.

2. Experimental layout

In order to experimentally characterize the ORC-based power unit and to compare the performance achieved by the unit with scroll expander and SVRE a fully instrumented test bench was developed following the approach adopted in [26]. For sake of coherence with the experimental campaign in [26] R245fa (6 kg mass) is selected as the working fluid with the addition of ISO VG 68 POE oil (5 % mass) for lubrication and sealing purposes at the pump and the expander.

The test bench (Figs. 1 and 2) features a diaphragm pump (f) with a 6.1 cm^3 volume displacement driven by an asynchronous electric motor (e). The pump speed – and eventually the working fluid mass flowrate - is varied through an inverter (e). The working fluid is brought to a slight superheated state (0–15 °C of superheating degree ΔT_{SH}) in a plate heat recovery vapor generator (PHRVG) (a) and enters the expander (b). An electric motor converts the mechanical power into electric power. Downstream the expander the working fluid is cooled down to a slightly subcooled state by tap water in a plate heat exchanger (c) and prior to start the cycle over it is gathered in a 3 L tank (d) for mass flow rate fluctuations damping particularly at higher pump RPM. Water (135 L) in a pressurized unit for thermal energy storage (g) works as the hot source: its temperature profile under normal solar exposure is reproduced by a pair of 12 kW electric heaters (h). A regulation valve modulates the mass flow rate provided by a dedicated circulation pump and reproduces the variability of the thermal load at the evaporator: when the DHW demand increases the regulating valve is closed thus reducing the availability of thermal power for the ORC-based power unit [26].

Thus both plant configurations employing SVRE (Fig. 1a) and hermetic scroll (Fig. 1b) machines are the same except for expander layout. Indeed the two machines present the same hydraulic scheme but due their technology nature have a different interface with the electric generator.

In the SVRE configuration (Fig. 1a and Fig. 2(d)) the expander is connected via flexible joints (s) to a torquemeter (l) – for measurement of the mechanical torque and expander RPM - and an asynchronous electric generator (r). A regenerative inverter introduces (r) the additional degree of freedom of expander RPM variation for regulation purposes providing the room to compare this approach to unit regulation to the one in Fig. 1b where the expander speed cannot be varied. The scroll configuration (Fig. 1b and Fig. 2(b)) accounts for a hermetic scroll expander (whose intake volume is 12.4 cm^3). The scroll shares with the electric generator (r) the same shaft and it is connected to a resistive electric load (q): the expander revolution speed is neither set by the electric grid nor controlled through an inverter but rather results from the dynamic equilibrium of the shaft. In order to measure the electric power a Wattmeter (t) was installed whereas the shaft revolution speed was evaluated via a magnetic probe connected to an oscilloscope (n). In Fig. 2(c) the fixed and orbiting Scroll configuration is reported.

The spirals are driven by a revolving shaft and perform axial intake (via the central port on the fixed scroll) expansion and exhaust circumferential discharge (port on the scroll). Pressure transducers and thermocouples placed upstream and downstream each component provide the values of the thermodynamic variables for cycle reconstruction. Magnetic flowmeters and Coriolis flow meters monitor the mass flow rate of water and working fluid. Concerning the SVRE (Fig. 2(e)) a whole cycle takes place within one complete rotation of the vane. Both intake and exhaust port are radial. More specifically the radial positioning of the intake port assures that the area for fluid transit is large enough to keep the fluid velocity low and the intake pressure high: this prevents the deterioration of the indicated cycle due to lower intake pressures and narrows the jet impingement-related losses. Table 1 summarizes the measurement uncertainties.

It is worth noticing that despite SVRE and Scroll presents different volume size revolutions speed range and electric generator connection they can be considered comparable solutions for the application at hand. Indeed the combination of different sizes and revolutions speeds ensures that the two machines elaborate the same mass flow rate for similar operating condition (expander intake pressure and temperature and expander exhaust pressure). As reported in Table 2 the Scroll machine displaces a volume of 12.4 cm^3 during intake phase whereas the intake volume of SVRE is 21.7 cm^3 (considering that the chambers are 7 and the intake volume of a single chamber is equal to 3.1 cm^3 (Fig. 2(e)). Hence the intake volume of SVRE is two times the one of Scroll machine.

Nevertheless in terms of flow rate delivered the higher Scroll revolution speed and higher volumetric efficiency guarantee that the two machines elaborate the same mass flow rate. Indeed considering the mass conservation equation at expander intake Eq. (1) can be written [24]:

$$\dot{m}_{wf} = \frac{\rho_{exp,in} V_{exp,in} \omega_{exp}}{\eta_{vol}} \quad (1)$$

where $\dot{m}_{wf}$ is the mass flow rate elaborated by the expander for certain density of working fluid at expander inlet $\rho_{exp,in}$ intake volume $V_{exp,in}$ expander speed ω_{exp} and volumetric efficiency η_{vol}.

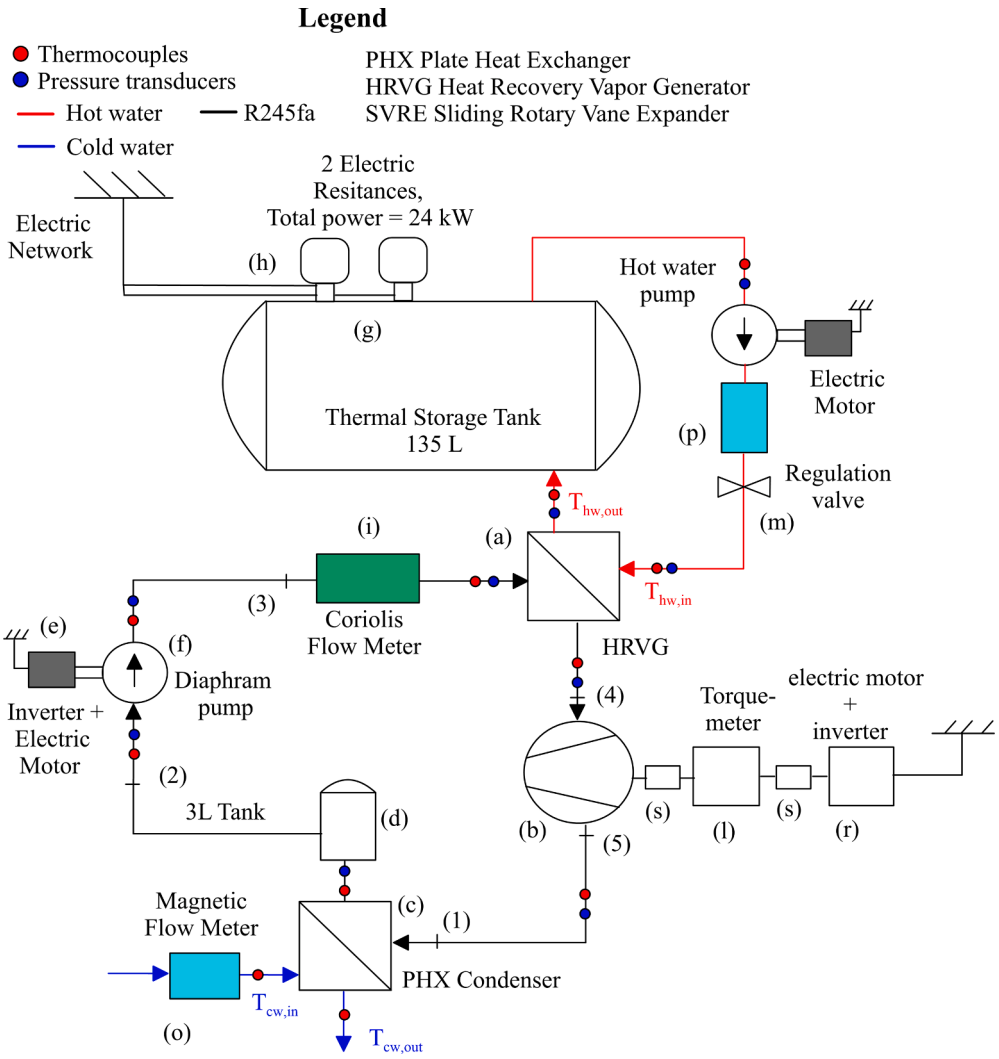

Fig. 1a. ORC-based power unit with SVRE schematics.

In design conditions the revolution speed of SVRE is 1500 RPM whereas the Scroll one results equal to 4000 RPM. Considering the volumetric efficiency the rated value of SVRE is 0.5 while the one of scroll expander is 0.8. These values ensures that both expanders elaborate the same mass flow rate for the similar operating condition reported in Table 2. This involves the fluid-dynamic similarity of the two devices. Despite this aspect the performances of the two devices for the considered application are generally different due to the variation of the global overall efficiency. Moreover the different operation of the two expanders leads to dissimilar operating range covered by the two machines.

As claimed above the different layout is called by the properties of the two technologies studied. A hermetic scroll expander encloses in the same casing the spirals and the generator making impossible the installation of torquemeter through dedicated joint as it has been done for the SVRE. The adoption of the same layout is of course possible as in [27–29] where the scroll expander is not hermetic and is connected to an external generator through joints via a torque-meter. On the other hand a hermetic scroll has been compared to hermetic or semi-hermetic SRVE [30]. It is clear as a hermetic machine is more reliable easy to be managed and installed.

In this paper the reference to the two expanders answers to different conceptual needs. Main common theoretical concept is the one which stresses the importance of the permeability of the plant and its modification when working fluid flow rate is changed driven by the entity of the recovery form the hot source. Permeability influences the maximum plant pressure and so the performance of the recovery unit. When a SVRE has been considered this paper outlines the effect of the speed variation done independently form the flow rate.

This offers an excellent degree of freedom to the maximum plant pressure control but requires dedicated electronics which make more complex and expensive the recovery units unmatching the simplicity the robustness and the cost reduction which are fundamental for the success of these units. When a scroll has been considered this paper made reference for the same reasons to a hermetic simple solution which loses the degree of freedom related to the revolution speed (whose variations depend on the working fluid flow rate). In spite of this limitation the scroll machine demonstrated fully suitable with energy performances even greater.

3. Performance analysis of the ORC-based power unit with a Scroll Machine

3.1. Expander and ORC-based power unit experimental characterization

The first step of the experimental analysis aims to the characterization of the scroll expander and ORC-based power unit performance (Fig. 3). The global efficiency of the expander is expressed as the ratio between the electric power produced by the expander and the reference power produced in case of an ideal adiabatic-isentropic expansion of the

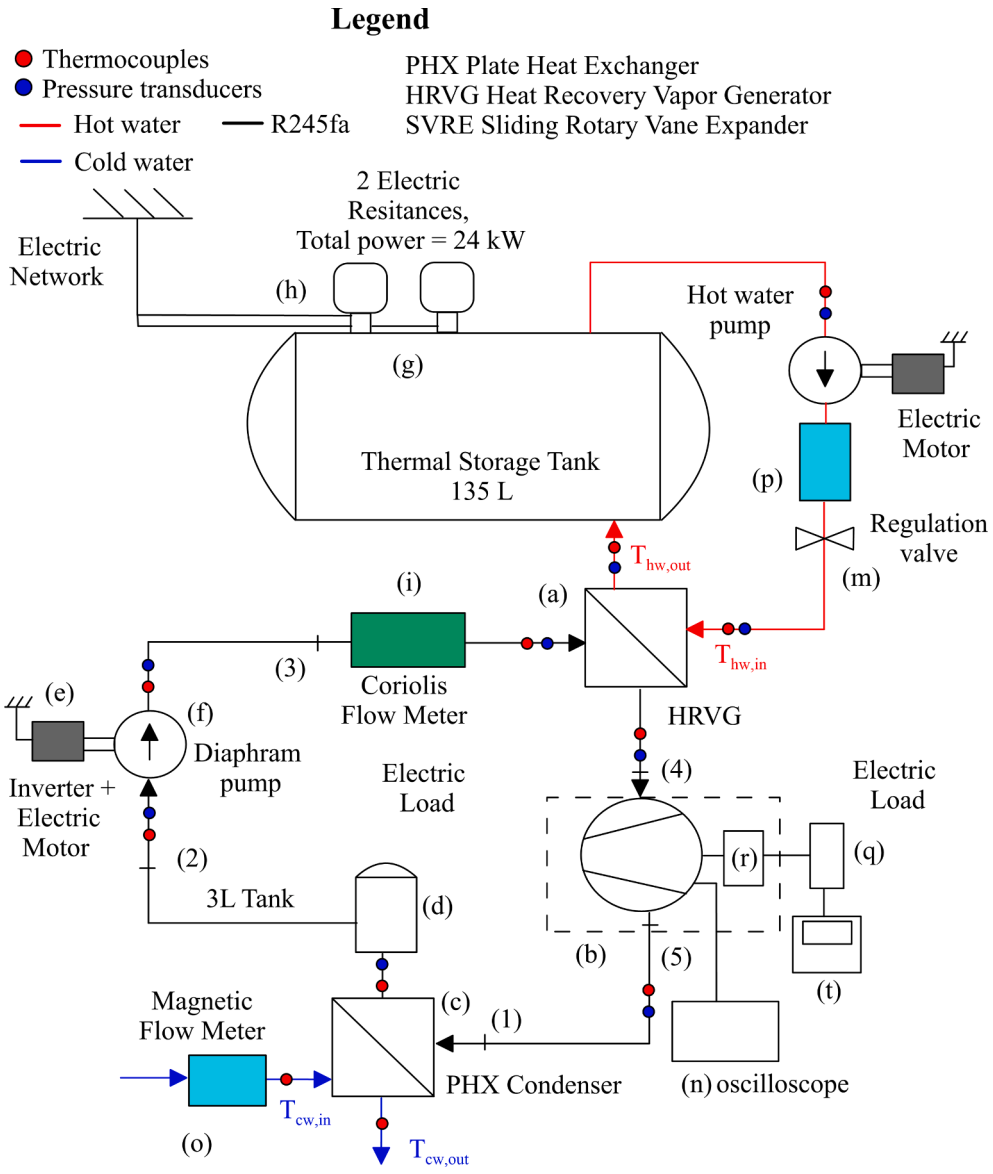

Fig. 1b. ORC-based power unit with scroll schematics.

machine Eq. (2) [29].

$$\eta_{exp} = \frac{P_{exp}}{P_{ad,is}} = \frac{P_{exp}}{\dot{m}_{wf}\left(h_{exp,in} - h_{exp,outis}\right)} \tag{2}$$

Therefore this efficiency also includes the conversion loss associated to the transformation of mechanical power produced by the scroll into electric power through the generator: Fig. 3(a) shows higher values than those expected from volumetric machines in similar scale applications and points out that the efficiency decreases from 60 % to 37 % when the mass flow rate grows from 17 g/s to 62 g/s. The volumetric efficiency defined as the ratio between the theoretical mass flow rate elaborated by the machine and the real one (Eq. (1)) - quantifies the impact of flow losses (i.e. the flow leakages from radial and flank gaps) on the expander power: the flow that by-passes the intake chamber and directly flows to the discharge port does not participate to power production so volumetric losses also present an energetic nature.

The expander volumetric efficiency (Fig. 3(b)) grows with the increasing mass flow rate: this result is not straightforward and depends on the expander intake volume $V_{exp,in}$ (i.e. 12.4 cm^3 each shaft revolution). At low mass flow rates the scroll is undercharged which depresses the volumetric efficiency. Moreover as the mass flow rate grows the expander pressure ratio raises (Fig. 3(c)): the volumetric efficiency suffers from higher characteristic pressure differences among the intake and exhaust side typically associated with larger volumetric losses especially at fixed RPM for the expander [24]. In the case at hand the expander is not operated at fixed revolution speed: it resets based on the dynamic configuration of the shaft i.e. depending on the equilibrium between the driving and resisting torque on the shaft. Nonetheless as the mass flow rate increases the expander pressure ratio increases and eventually the expander driving torque and expander RPM increase (Fig. 3(e)). Thus the increase of the expander speed which follows a univocal growth path leads to an improvement of the sealing capacity of the machine that consists of two eccentric scrolls. As a matter of fact the negative effect of the pressure ratio growth is overwhelmed by the expander speed raise.

The improvement of the volumetric efficiency with the mass flow rate suggests that the power reduction with the mass flow rate is due to the losses related to dry and viscous effects. This can be demonstrated by integrating Eq. (1) with Eq. (2) into Eq. (3) [24]:

$$\eta_{exp} = \frac{P_{exp}}{\dot{m}_{wf}\left(h_{exp,in} - h_{exp,out_{ad,is}}\right)} = \frac{P_{exp}}{\dot{m}_{th}\left(h_{exp,in} - h_{exp,out_{ad,is}}\right)}\eta_{vol} \tag{3}$$

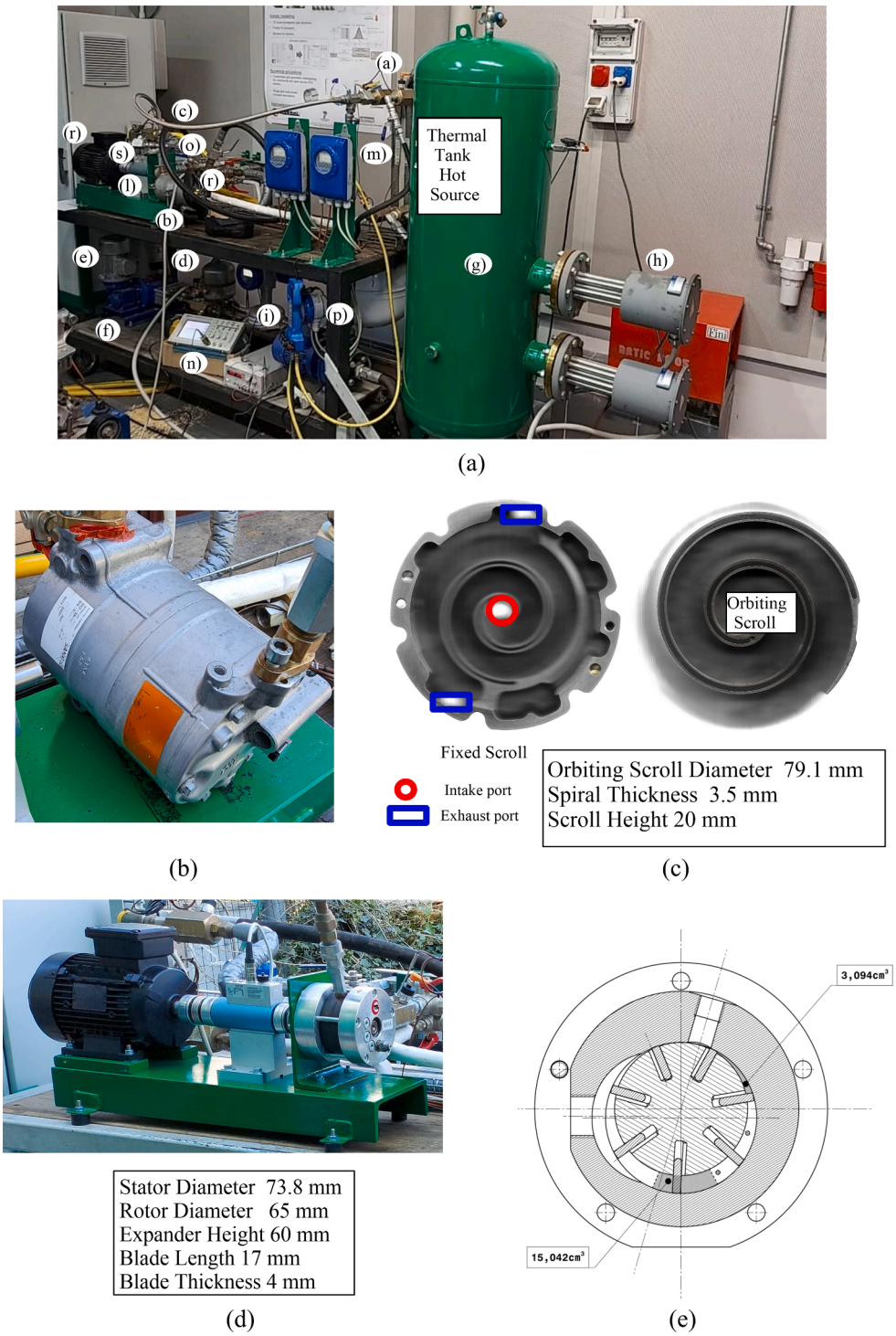

Fig. 2. ORC unit (a) Scroll expander configuration (b-c) Sliding Rotary Vane Expander configuration (d-e).

The expander efficiency depends on the volumetric efficiency: as the mass flow rate increases the pressure ratio increases leading to larger frictional losses and eventually to a penalty on the global efficiency.

Despite global efficiency decreases in the observed mass flow rate interval the expander power shows a growing trend from 150 W to 530 W. The increase of power with mass flow rate is basically due to the enhancement of the pressure ratio across the machine: the higher the pressure ratio the larger the indicated power and eventually the net power generated. Both the indicated power and the mechanical power lost to friction and viscous effects increase with the mass flow rate enhancement: the indicated power shows a more marked growth than the power lost. This explains the quite linear increase of expander power as function of the mass flow rate. It is worth noticing that the scroll expander presents a built-in volume ratio equal to 2 thus an increase of the pressure ratio provides the growth of impact of isochoric expansion at the start of the discharge phase. This is the main cause of the global efficiency reduction in accordance with what observed in [26].

A more precise evaluation of this phenomenon can be achieved with an experimental measurement of the indicated cycle. Nevertheless the indicated cycle is hard to measure in scroll machines due to the complex

Table 1
Measurement uncertainties.

Variable	Sensor Type	Measurement uncertainty
Temperature	Thermocouple	± 0.75 °C
Pressure	Pressure transducers	± 1.5 % of full-scale
Mass flow rate (R245fa)	Coriolis Flow meter	± 0.15 % measured value
Mass flow rate (water)	Magnetic Flow meter	± 0.5 % measured value
Power	Wattmeter	± 1 % measured value
Torque	Torque-meter	± 0.2 Nm
Revolution speed	Torque-meter	± 1 rpm
ORC efficiency (scroll case)		1.7 %
ORC efficiency (SVRE case)		1.1 %
ORC Net Power (scroll case)		1.4 %
ORC Net Power (SVRE case)		0.6 %

configuration and geometry. Moreover to the Authors' best knowledge the scientific literature would not provide any experimental result on the indicated cycle for scroll expander to use for comparison anyway. Plus the present work sticks to the experimental characterization of the impact of expander behavior on the whole plant performance leaving any effort on the indicated cycle assessment to future development.

Fig. 4(a) shows that the expander power affects the net power output of the whole ORC plant which increases with mass flow rate up to 450 W. On the contrary the ORC plant shows a linear decrease with mass flow rate enhancement: as the mass flow rate increases the expander efficiency sensibly decreases due to the higher mechanical and isochoric expansion losses confirming that both plant power and plant global efficiency depend on the expander behavior.

3.2. Analysis of impact of scroll expander behavior on ORC plant operating condition

The expander behavior plays a strong role in the definition of the ORC maximum pressure i.e. the expander intake pressure net the pressure drops between the evaporator and the expander. In volumetric machines the expander intake pressure depends on the machine permeability expressed as the ratio between the mass flow rate entering the expander and the pressure difference between the intake and exhaust sides (Eq. (4)) [24]:

$$\alpha = \frac{\dot{m}_{WF}}{\Delta p_{exp}} \tag{4}$$

Where the pressure difference is expressed referring to the expander intake and exhaust values [24]:

$$\Delta p_{exp} = p_{exp,in} - p_{exp,out} \tag{5}$$

For any given flow rate of the working fluid fed to the machine the lower the permeability the higher the pressure difference between the expander intake and exhaust side. Hence as the expander exhaust pressure basically depends on the cold source condition the permeability defines the intake pressure of the expander and consequently the maximum plant pressure. Thus the predictability of permeability effects is key to develop a detailed theoretical model to support a sound regulation strategy: such an approach already proved to be very effective in the case of a sliding vane rotary expander (SVRE) operated at constant revolution speed varied independently from the expander working conditions [24]. In the case at hand the machine configuration implies that the expander speed and the pressure ratio vary jointly. Consequently the residual degree of freedom for plant regulation is the variation of the mass flow rate of working fluid through pump speed modulation. The model should summon all these effects to assess the overall plant performance.

Fig. 5 reports the expander operating quantities as function of mass flow rate and pressure ratio with the superheating degree as a parameter. The expander intake pressure has a linear growth from 5 bar to 12 bar when the mass flow rate increases from 17 g/s to 70 g/s independently from the superheating degree (Fig. 5(a)): unexpectedly a similar trend is retrieved in applications where a constant revolution speed is considered [24]. Differently from the expander intake pressure the exhaust pressure (Fig. 5(b)) shows a weak linear growth thus it can be considered constant for a general analysis: the growth of pressure ratio with mass flow rate (Fig. 5(c)) is basically defined by the trend of the intake pressure. Fig. 5(d) and (e) report the variation of expander speed with the mass flow rate and the pressure ratio respectively. The growth trend is similar because the pressure ratio which defines the expander speed variation follows a linear increase with the mass flow rate. The effect in terms of enhancement of the volumetric efficiency is appreciated in Fig. 5(f) along with the negligible dispersion of points with respect to the linear trend.

Considering this experimental evidence the permeability concept can be defined for this expander configuration. The starting point is the volumetric efficiency equation analogous to [24]. Thus from Eq. (2) the density can be outlined (Eq. (6)) and introduced in the ideal gas law corrected through the compressibility factor obtaining the intake pressure (Eq. (7)) [24].

Table 2
Flow rate delivered by the Scroll and SVRE machines.

		Scroll	SVRE
Properties			
$V_{exp,in}$	cm^3	12.4	21.7
ω	RPM	4000	1500
η_{vol}	η_{vol}	0.8	0.5
Expander layout and set-up			
	Expander/Generator connection	Enclosed in the same machine casing; Shares the shaft with the scroll; Connected to a dissipative electric load.	The connection with expander is performed through joints; Has a different shaft with respect to the expander; Connected to the electric network through a regenerative inverter.
	Revolution speed	Defined by the equilibrium on the expander shaft.	Externally imposed through the regenerative inverter.

Operating conditions

$P_{exp,in}$ [bar]	$T_{exp,in}$ [°C]	$\dot{m}_{WF}$ [g/s]	$\dot{m}_{WF}$ [g/s]
6	79	34.3	32.6
7	85	39.9	38.0
8	91	45.7	43.5
9	95	51.5	49.1
10	100	57.4	54.7
11	104	63.4	60.4
12	108	69.5	66.2

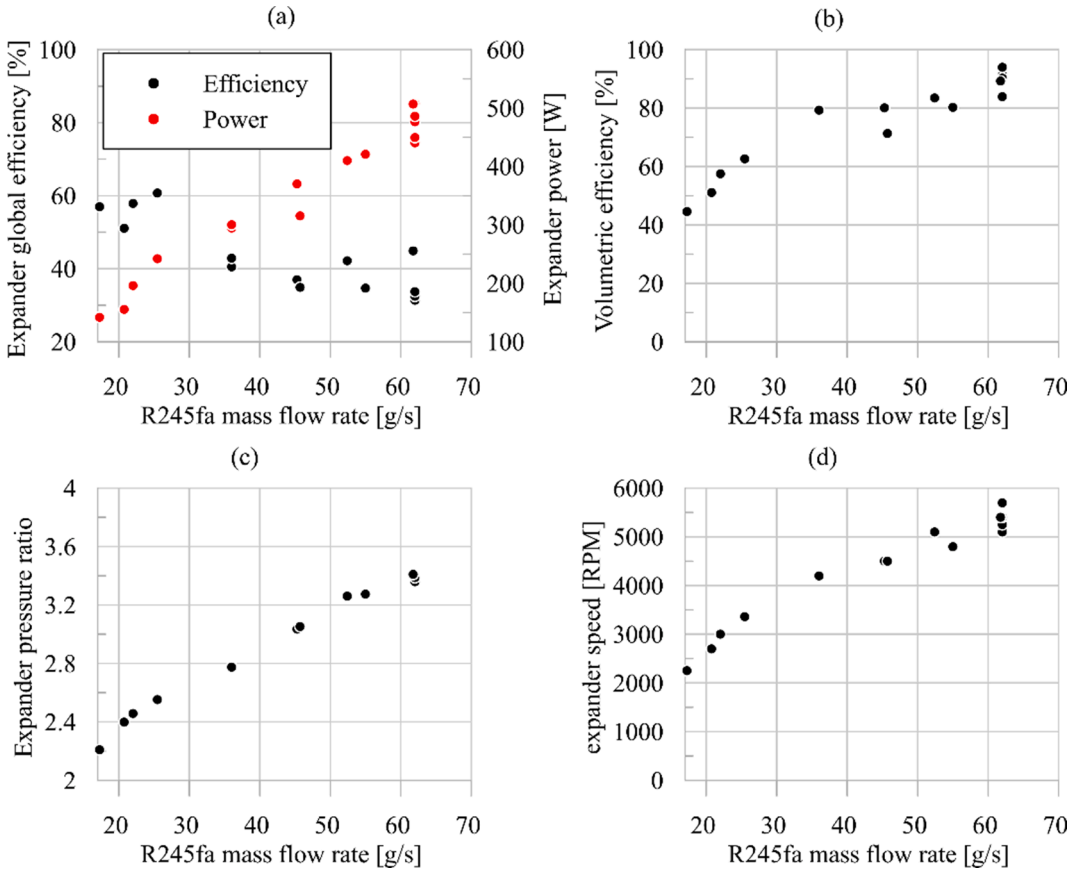

Fig. 3. Power and Global(a) and volumetric efficiency (b) pressure ratio(c) and speed of the expander(d).

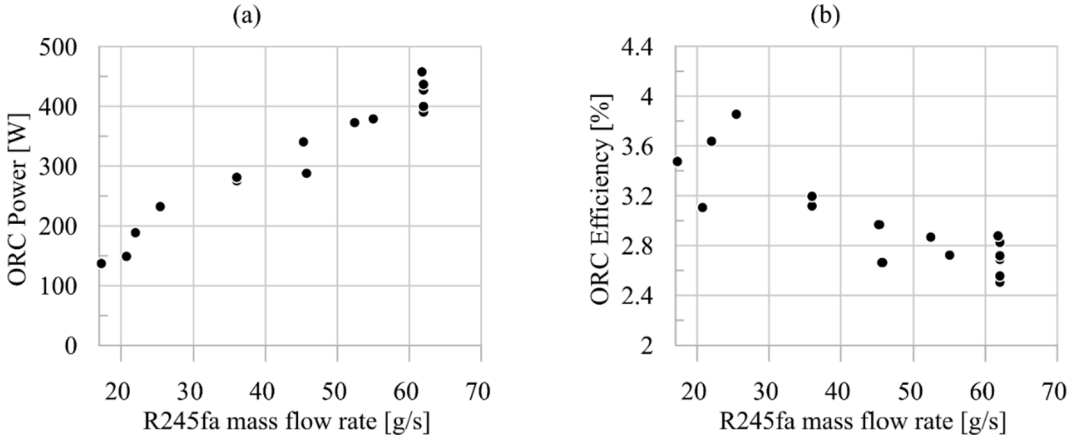

Fig. 4. Power (a) and efficiency (b) of ORC-based power unit.

$$\rho_{exp,in} = \frac{\dot{m}_{wf}\eta_{vol}}{V_{exp,in}\omega_{exp}} \tag{6}$$

$$p_{exp,in} = ZRT\frac{\dot{m}_{wf}\eta_{vol}}{V_{exp,in}\omega_{exp}} \tag{7}$$

Eq. (7) is the general equation of permeability and applies to the case described in [24]. The loss of the revolution speed as independent variable reduces the degrees of freedom to rely on for plant control but results in a simpler relation between the plant operating conditions. As a matter of fact the revolution speed can be represented by a linear function (Eq. (8)) obtained by fitting the experimental data:

$$\omega_{exp} = k'\dot{m}_{wf} + q' \tag{8}$$

Also the relation between the volumetric efficiency and the other operating conditions can be simplified. In the case at hand the mass flow rate rules the variation of pressure ratio and revolution speed. Therefore the volumetric efficiency can be represented as mass flow rate dependent (Eq. (9)). This relation could be approximated with a linear function for a preliminary analysis:

$$\eta_{vol} = k''\dot{m}_{wf} + q'' \tag{9}$$

Thus introducing (8) and (9) in (7) the novel form of permeability equation can be achieved (10):

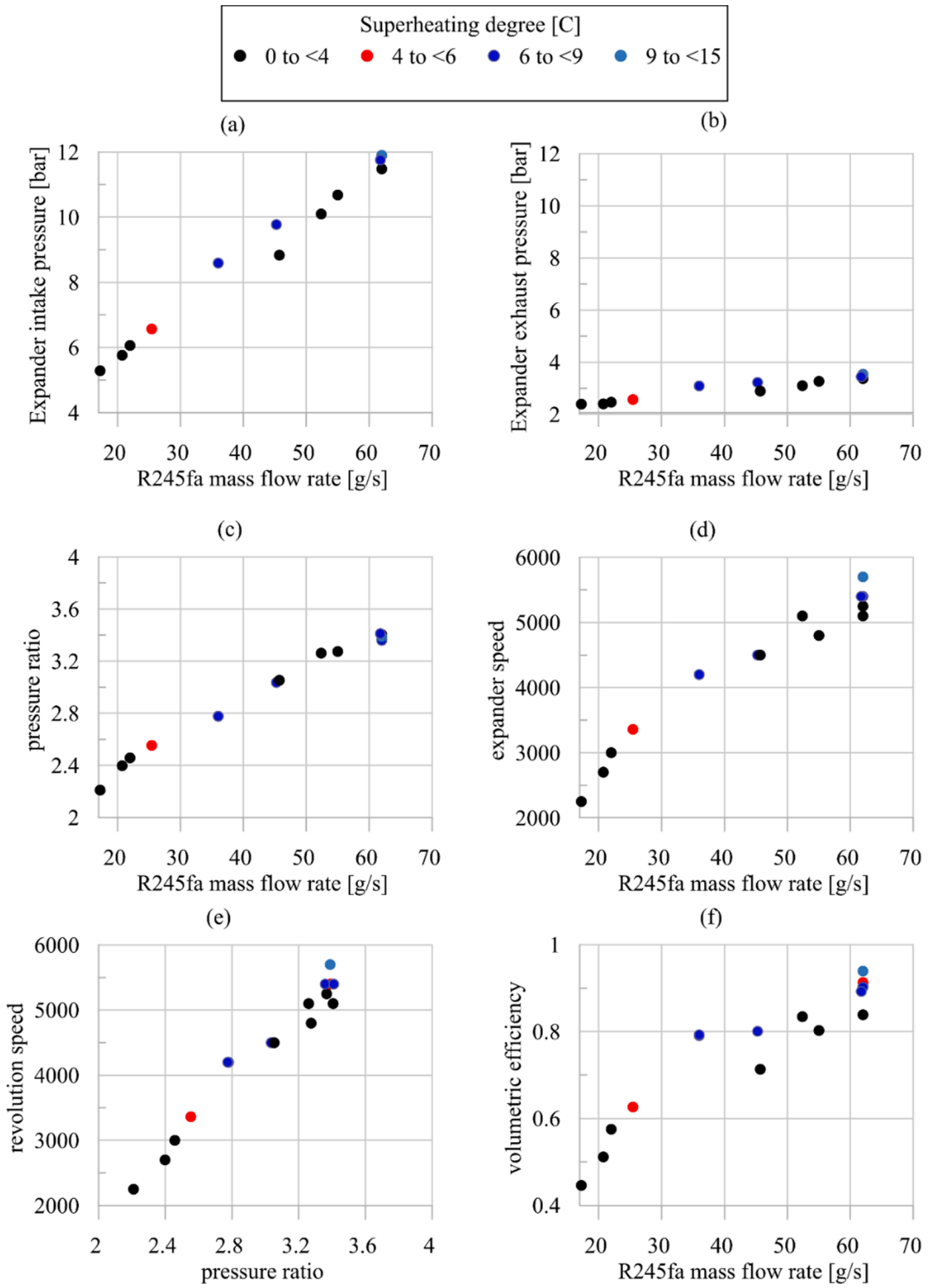

Fig. 5. Intake pressure (a) exhaust pressure (b) pressure ratio (c) and speed (d) of the expander as function of mass flow rate; speed (e) and volumetric efficiency (f) of the expander as function of the pressure ratio.

$$p_{exp,in} = ZRT\frac{\dot{m}_{wf}(k''\dot{m}_{wf} + q'')}{V_{exp,in}(k'\dot{m}_{wf} + q')} = K'\dot{m}_{wf} \tag{10}$$

Hence Eq. (10) shows that pressure and mass flow rate can be linked by a linear relation in accordance with the experimental evidence. Dividing both terms of Eq. (10) for exhaust pressure preliminary considered as a constant value the pressure ratio trend can be obtained Eq. (11):

$$\frac{p_{exp,in}}{p_{exp,out}} = \beta = \frac{K'\dot{m}_{wf}}{p_{exp,out}} = K''\dot{m}_{wf} \tag{11}$$

Nevertheless as observed in [24] Eq. (10) cannot be solved in a closed form because the temperature and pressure are univocally related. For this reason the same iterative procedure described in [24] was adopted with the additional complexity of the revolution speed no longer being an independent variable (Fig. 6).

The main steps of the adopted procedure can be recognized in Fig. 6:

(1) The mass flow rate provided by the pump was adopted to evaluate RPM according to the experimental fitting.
(2) The mass flow rate allows to evaluate also the volumetric efficiency according to the experimental correlation.
(3) These parameters are introduced in the permeability equation obtaining the intake pressure of the expander and consequently the pressure ratio.
(4) Permeability equation however is not linear thus at step 0 an initial value of the temperature should be introduced. The mass flow rate is the main driver of the intake pressure growth and the temperature does not significantly affect this parameter. Thus the selection of the initial value does not require constraints.
(5) For sake of model accuracy the temperature was updated through an iterative procedure. First the initial temperature T_0 and in general the value corresponding at the i-1-calculation step is compared to the saturation temperature corresponding to the intake pressure evaluated from step (3) plus the 5–10 °C superheating degree. This latter value was called T_i. If the absolute difference is lower than a prescribed tolerance the evaluation ends providing the experimental pressure otherwise T_i replace the T_{i-1} value in (3).

The calculation converges in few iterations and provides the intake pressure and consequently the pressure ratio. The novel permeability model was validated comparing its predictions against the experimental data and the comparisons are reported in Fig. 7. The prediction and the experimental data in terms of intake pressure are in good agreement (Fig. 7(a)) with a 10.2 % max deviation and a 6.05 % Root Mean Square Error. Similar results are appreciated on the expander intake temperature (Fig. 7(b)) with a 10.7 °C maximum absolute error on the intake temperature and a 4.6 °C corresponding average error. Therefore the accuracy of the present model can be retained fully satisfactory considering its simplicity and low computational cost. The model development indicates a clear strategy for the unit control only based on the mass flow rate variation. In fact the expander revolution speed is not an independent control parameter due to its configuration. This leads to a simpler control logic but at the same time the loss of the expander speed control prevents the possibility to vary the intake pressure for a given mass flow rate.

The experimental results reported in Figs. 5 and 7 show that despite the revolution speed varies in a wide range (2000–6000 RPM) the pressure ratio sees a quite linear trend as in the case of constant revolution speed. Based on (11) - whose numerator and denominator are the volumetric efficiency and revolution speed respectively - even if the expander revolution speed is not fixed as a control parameter but rather results from a dynamic equilibrium the global dependence of intake pressure (and consequently of pressure rise) with mass flow rate is linear as in the case of constant speed. In particular when the mass flow rate of working fluid increases both revolution speed and volumetric efficiency shows a quite univocal linear growth.

Therefore it can be concluded that from a permeability point of view there is no difference between the case of constant revolution speed and the situation where the expander revolution speed is unconstrained. On the other hand if the revolution speed is externally imposed the permeability is not univocal anymore and varies with it. More specifically if the revolution speed increases for a given mass flow rate the intake pressure and pressure ratio decrease whereas for a revolution speed reduction these pressure parameters grow. This case is faced in the following when the SVRE case is addressed.

4. Performance analysis of the Sliding Rotary Vane Expander set-up

4.1. ORC-based power unit with a Sliding Rotary Vane Expander

Since it can be modulated via the regenerative inverter the expander revolution speed adds to the pump speed as unit control variable. The pump speed fixes the working fluid flow rate and allows to adapt it to the available thermal power at the evaporator. The expander speed is instead related to the intake pressure and the pressure ratio of the expander. Indeed the revolution speed control allows to change the machine permeability broken the unicity of the pressure versus mass flow rate increase corresponding to a constant revolution speed situation [24]. It is important to observe that the variation of revolution speed is not sufficient to decouple the pressure behavior from the mass flow rate variation. In fact it is fundamental that the revolution speed value is set as an independent parameter kept constant in presence of mass flow rate and consequently expander pressure ratio excursion. Indeed in the scroll configuration the revolution speed depends on the operating conditions and it is not set as an independent parameter and the intake pressure

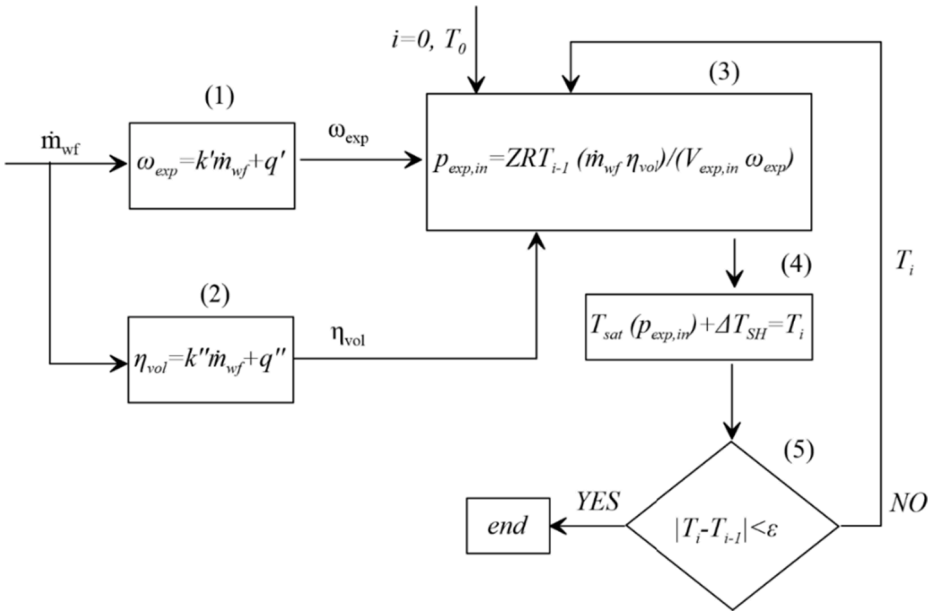

Fig. 6. Scheme of the permeability model.

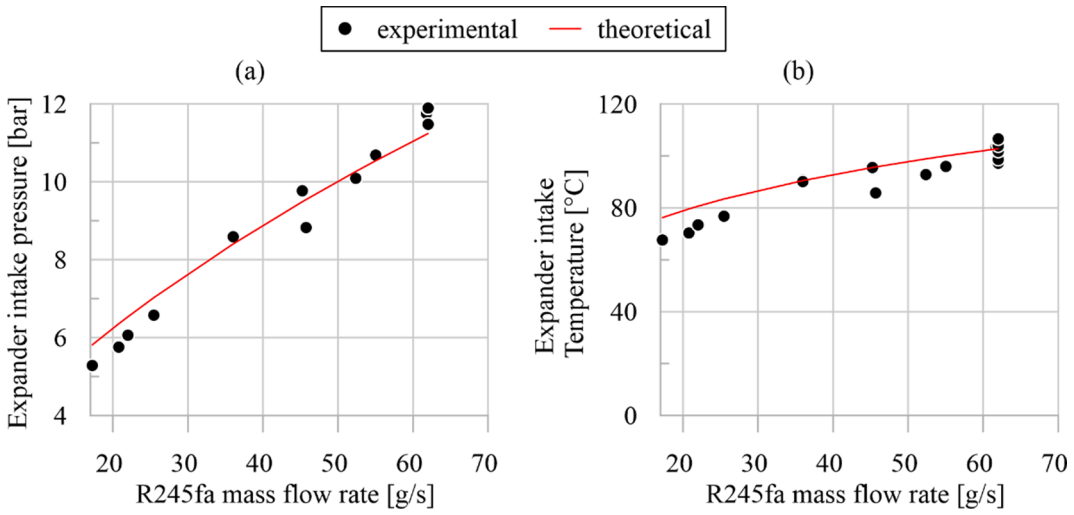

Fig. 7. Comparison between experimental data and theoretical results.

raises as a function of mass flow rate following a univocal path (Fig. 5 (a)). This can be analytically demonstrated observing Eq. (10) where the dependence of revolution speed on expander intake pressure is lost ω_{exp} being linearly dependent on the mass flow rate. In the case of Sliding Rotary Vane expander being ω_{exp} an independent parameter the intake pressure variation with mass flow rate is ruled by Eq, (7). Eq. (7) clearly

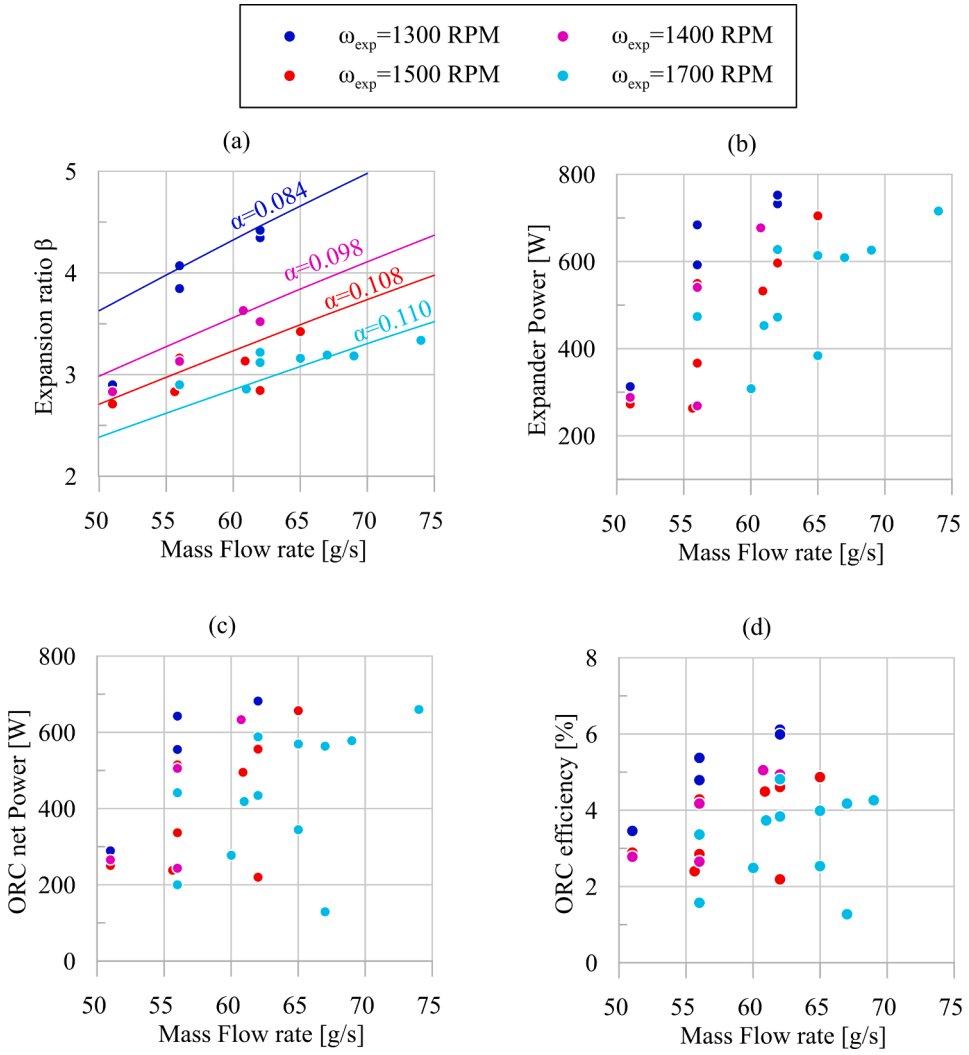

Fig. 8. Expansion ratio and permeability [kg/(MPa)](a) expander power (b) net orc-based unit power (c) and orc-based unit efficiency (d) as function of mass flow rate and revolution speed.

shows that varying ω_{exp} the relation between mass flow rate and intake pressure changes leading to multiple growing paths. This phenomenon depends on the permeability variation of the expander which depends also on revolution speed [24]. Introducing Eq. (7) in Eqs. (5) and (4) permeability can be expressed as function of the expander operating parameters (Eq. (12)) [24]:

$$\alpha = \frac{\dot{m}_{WF}}{\left(ZRT\frac{\dot{m}_{wf}\eta_{vol}}{V_{exp,in}\omega_{exp}} - p_{exp,out}\right)} \tag{12}$$

The permeability increases with the growth of expander intake volume and revolution speed whereas diminishes with increase of volumetric efficiency. Thus concerning the effects of the revolution speed on the permeability the higher its value the lower the pressure difference at expander side for a given flow rate of working fluid. On the other hand decreasing the revolution speed the permeability of the machine diminishes leading to a larger pressure difference at the expander sides keeping constant the mass flow rate (Fig. 8(a)): the expansion ratio – i.e. the expander intake pressure divided by the exhaust pressure - follows a quite linear growth with the mass flow rate enhancement. Moreover the slope of the linear trend decreases with the increase of the revolution speed. The increase of the revolution speed in fact produces an increase of permeability which ranks from 0.084 kg/MPa to 0.110 kg/MPa when the revolution speed grows from 1300 RPM to 1700 RPM. The linear trend is associated with a 10 °C superheating: experimental points that refer to a different value of superheating return close-to-linear trends. This confirms that the main driver of the expansion ratio growth is the mass flow rate enhancement and the expander revolution speed value in line with the theoretical expectations in [24]. From a regulation perspective an extended expander operability can be attained making the plant suitable to different values of thermal power at the evaporator i.e. to different values of mass flow rate of working fluid processed by the pump: for low mass flow rates a low revolution speed (1300 RPM) ensures to reach larger expansion ratios (4–4.5) achieving a 600 W-750 W expander power (Fig. 8 (b)) a 550 W-700 W ORC Net Power (Fig. 8(c)) and a 5–6 % efficiency (Fig. 8(d)). With a larger thermal power availability the expander RPM is increased up to 1700 RPM to set a suitable expansion ratio (3.3) that corresponds to 75 g/s mass flow rate: a 660 W Net ORC power is achieved with a 4 % efficiency.

4.2. Effects of revolution speed variation on expander performance

As previously observed the expander permeability can be varied acting on expander revolution speed i.e. the expansion ratio at the expander can be adapted to any given flow rate entering the machine with obvious effects on the ORC unit control. In particular as the expander speed diminishes the permeability decreases and the expansion ratio at the given flow rate grows. This peculiarity can be exploited to regulate the unit enhancing the expander and ORC operability: when the mass flow rate entering the machine is lower with respect to the design value the optimal value of the pressure ratio at the expander can be reached by reducing the revolution speed.

In Fig. 9(a) it can be observed that the expander revolution speed increases quite linearly with the mass flow rate processed by the pump depending on the available thermal power at the evaporator. If the expander speed is constant the expansion ratio grows quite linearly with the mass flow rate. Nevertheless this situation could lead to too lower expansion ratio when the flow rate entering the expander drops. In this condition the expander cannot be operated and the ORC is switched off. On the other hand if the mass flow rate becomes significantly larger than the design value (60 g/s) the expansion ratio enhances. Consequently the intake pressure and the maximum plant pressure grows inducing more severe mechanical stress on the plant components.

To face the mass flow rate reduction with respect to the design value the revolution speed could be reduced (Fig. 9(a)) providing a larger expansion ratio for a given mass flow rate (Fig. 9(b)). For instance if the mass flow rate reduces from 60 g/s down to 55 g/s and both the expander speed is kept to its design value ($\omega = 1500$ RPM) the expansion ratio decreases from its 3.5 design value down to 2.9. Only a reduction in the expander down to 1300 RPM prevents the drop in the expansion ratio ($\beta = 4$).

On the other hand when the mass flow rate assumes its maximum value (75 g/s) if the revolution speed is kept constant to the design value the expansion ratio and consequently the intake pressure could reach unsafe value for the machine components integrity. Thus the increase of revolution speed ensures to reduce the expansion ratio providing a lower intake pressure. The detrimental effect of expansion ratio reduction on power production can be compensated by the revolution speed

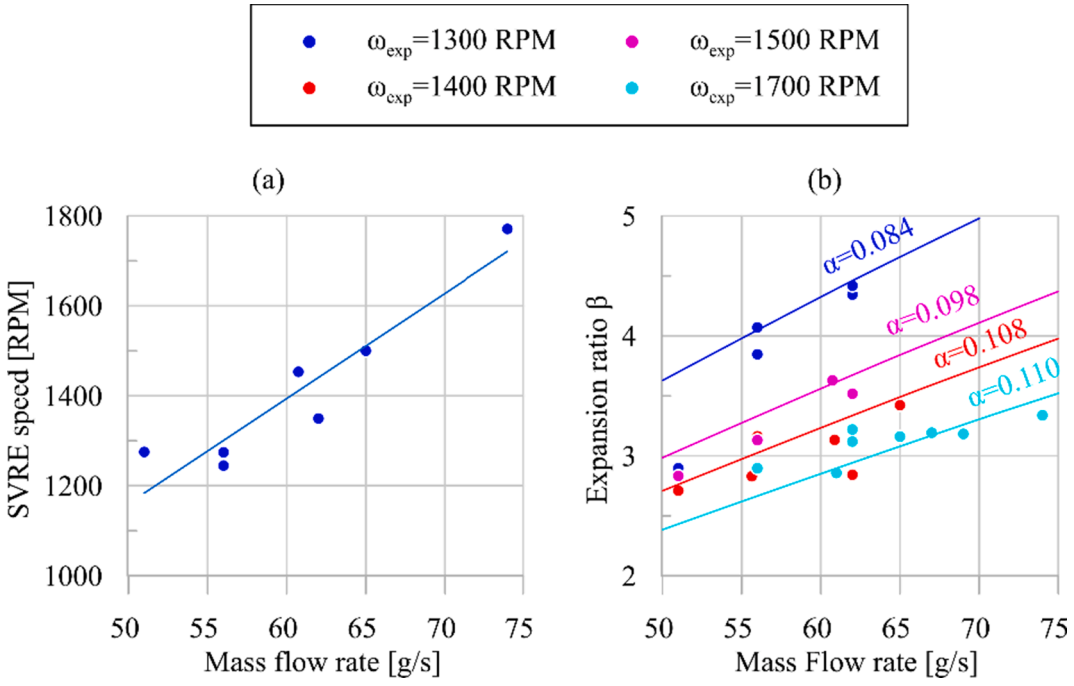

Fig. 9. Revolution speed (a) and expansion ratio (b) as function of mass flow rate.

enhancement leading to a larger number of cycles performed over time.

The revolution speed is one of the operating parameters which affects the expander performance the most [24]. Hence when the revolution speed was varied for regulation issues the expander power and efficiency variation should be considered.

As it can be seen in Fig. 10(a) the maximum power was produced in correspondence of the design speed (1500 RPM): any variation of this parameter would result in a lower power output. Indeed if the revolution speed decreases the machine works with a larger expansion ratio (Fig. 9 (b)) but performs less cycles per unit of time. On the other hand if the expander works at higher revolution speed more cycles are performed over time but the expansion ratio is lower. Moreover the increase of expander speed leads to a lower expander efficiency due to larger frictional losses (Fig. 10(b)). It is worth to observe that the curve assumes a flat trend when the speed varies between 1200 and 2000 RPM. Indeed the expander power and efficiency vary respectively between 600–700 W and 33–35 %. The trends of the ORC power (Fig. 10(c)) and ORC efficiency (Fig. 10(d)) as function of the expander revolution speed matches the trend of the expander power (Fig. 10(a)) and expander efficiency (Fig. 10(b)) being the offset due to the pump power absorption. The power and efficiency show a relatively flat trend when the expander speed varies between 1200 RPM and 2000 RPM. In this range the ORC power varies between 550 W and 650 W whereas the ORC efficiency between 4.2 % and 5.4 %. ORC efficiency was evaluated as the ratio between the ORC net power and the hot source (hot water) thermal power (Eq. (13)) [29].

$$\eta_{ORC} = \frac{P_{ORC}}{Q_1} = \frac{P_{exp} - P_{pump}}{\dot{m}_{hw}\left(h_{hw,in} - h_{hw,out}\right)} \tag{13}$$

The present analysis was not performed for scroll machine as the revolution speed is not a control parameter but it depends on the processed mass flow rate.

4.3. SVRE permeability model

In order to assess how to vary the expander speed to vary the expansion ratio (and consequently the expander intake pressure) a permeability model was developed. This task was performed in analogy to the one developed for scroll expander with the only exception that in the SVRE model the revolution speed (Step 2 in Fig. 11) is set as an independent value and it is not obtained through a linear correlation. The error between theoretical and experimental values of pressure and temperature at intake are in Fig. 12.

Considering the intake pressure (Fig. 12(a)) the Root Mean Square Error is equal to 3.6 % whereas the maximum deviation is 10.07 %. Meanwhile the intake temperature (Fig. 12(b)) presents a 10.2 °C maximum deviation and a 4.6 °C average absolute error. In the configuration discussed above the model already provides a satisfactory trade-off between accuracy simplicity and convergence speed. In case a linear growth of the volumetric efficiency with the revolution speed is considered the permeability equation (step 3 Fig. 11) is simplified along with the overall model: such an assumption applies to the case at hand because in spite of the volumetric efficiency dependence on the mass flow rate (Fig. 13(a)) the main driver for increasing the volumetric efficiency is the revolution speed which allows to neglect non-linearities between expander intake pressure and mass flow rate once the expander speed is set as an independent parameter.

The linear relation between the intake pressure and the mass flow

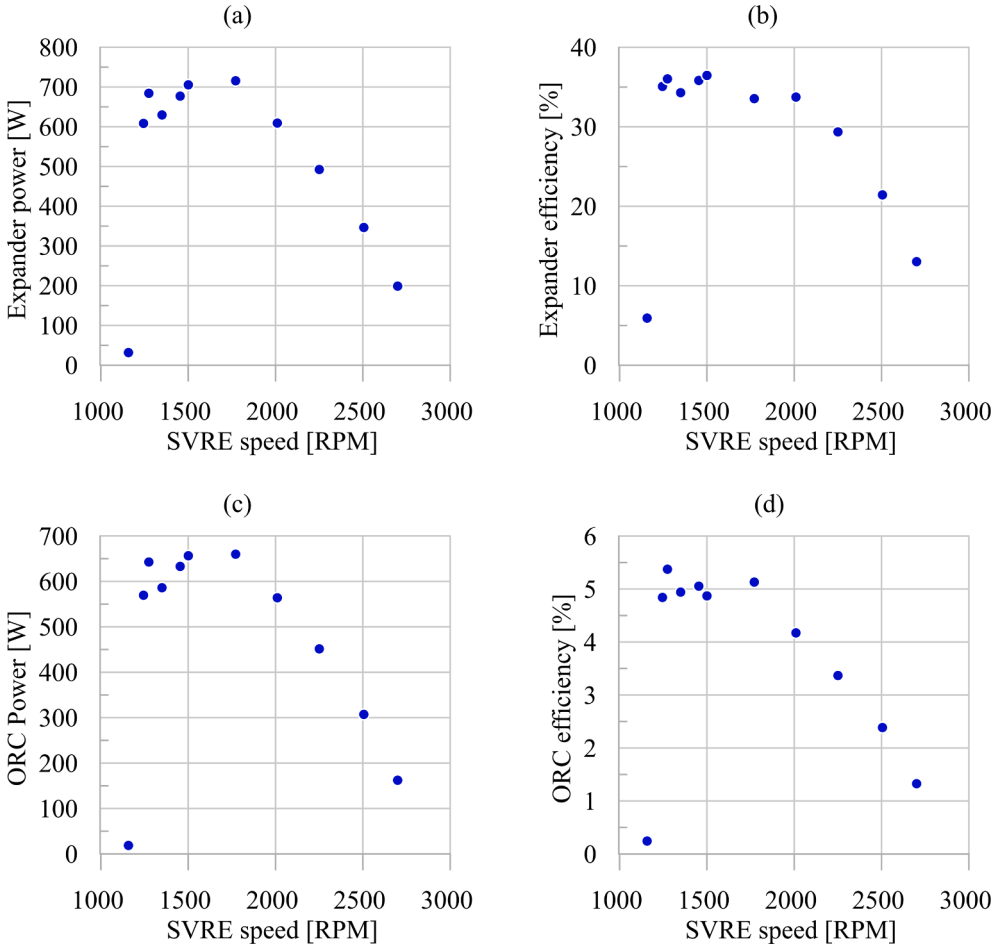

Fig. 10. Expander power (a) Expander efficiency (b) ORC power (c) and ORC efficiency (d) as function of SVRE revolution speed.

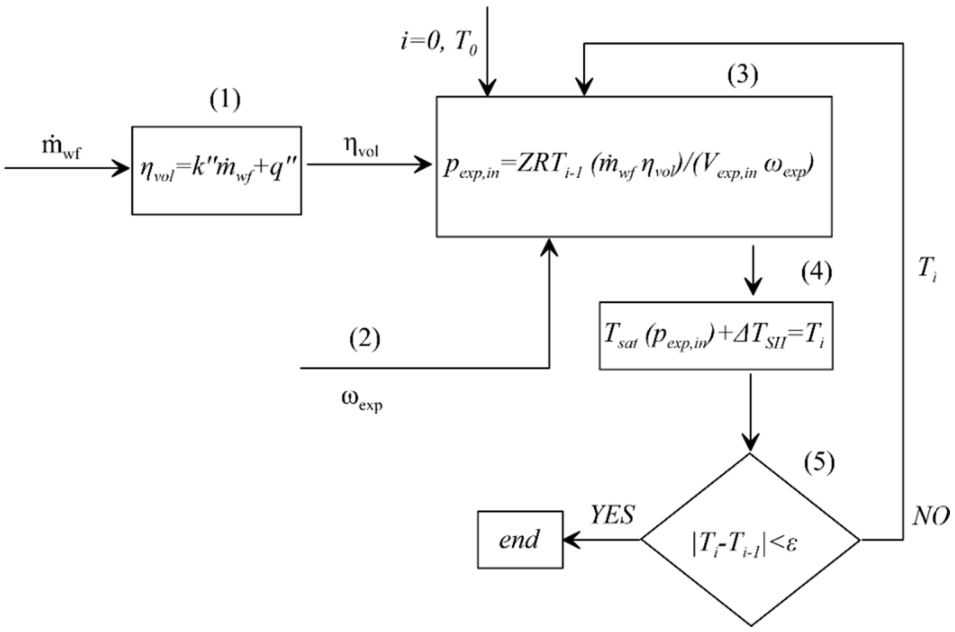

Fig. 11. Scheme of Sliding Rotary Vane Expander permeability.

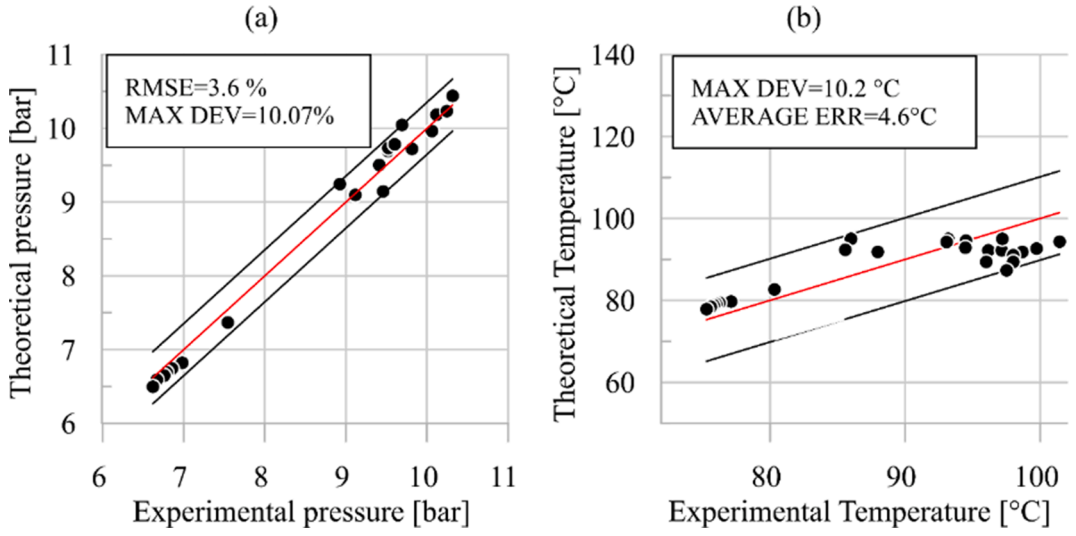

Fig. 12. Comparison between experimental and theoretical pressure (a) and temperature.

rate variation was confirmed by the good agreement between the experimental data and the theoretical prediction reported for 1300 RPM 1400 RPM 1500 RPM and 1700 RPM respectively in Fig. 13 (b) (c) (d) and (e). The different linear growth paths are shown in Fig. 13(f) which provides a regulation map to define the revolution speed at which the expander should rotate to achieve a certain intake pressure for a given flow rate set by the pump.

Therefore the adoption of the present model allows to simply address the issue of plant regulation without heavy numerical model. This represents an advantage in terms of computational cost and on the velocity in the definition of the new operating conditions. This latter aspect is particularly important considering that the expander is characterized by a fast dynamic behavior and affects the maximum plant operating pressure.

5. Comparison between scroll expander and SVRE performance

Once the SVRE was experimentally characterized its performances were compared with those of the Scroll machine. In Fig. 14 the comparisons in terms of expansion ratio (a) expander power (b) Net ORC power (c) and efficiency (d) were reported. Prior to discuss the different expander behavior it is worth noticing that the two machines are characterized by a different volumetric size. The Scroll machine has an intake volume of 12.4 cm^3 whereas the one of SVRE is 21.7 cm^3 (3.1 cm^3 for each vane). Nevertheless despite SVRE presents a higher intake volume Scroll expander presents a higher permeability due to the larger revolution speed (varying between 2000 RPM and 6000 RPM). For this reason the expansion ratio is lower for Scroll device which respect to that of the SVRE case keeping constant the mass flow rate provided by the pump (Fig. 14 (a)).

Due to the lower expansion ratio the Scroll Machine produces a lower power with respect to the SVRE case. However the power provided by the Scroll is lower if compared to the SVRE case despite a higher expansion ratio for the Scroll machine: with a 50–60 g/s mass flow rate the expander speed is comprised between 4500 and 6000 RPM for Scroll significantly higher than the one for SVRE (1700 RPM). Therefore the

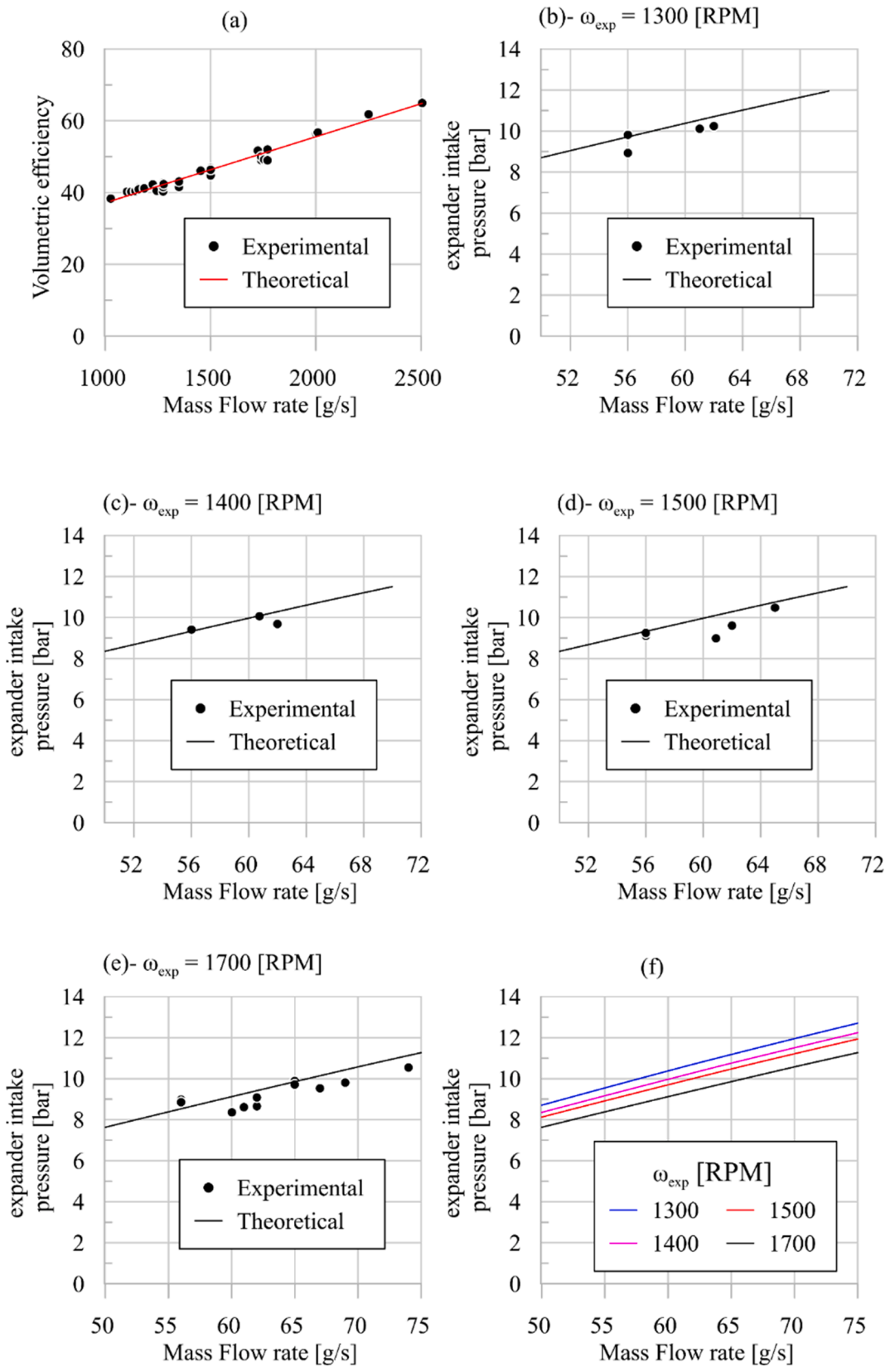

Fig. 13. Volumetric efficiency as function of revolution speed of SVRE (a); comparison between theoretical and experimental intake pressure value at 1300 RPM (b) 1400 RPM (c) 1500 RPM (d); Predicted intake pressure as function of mass flow rate for different expander speed.

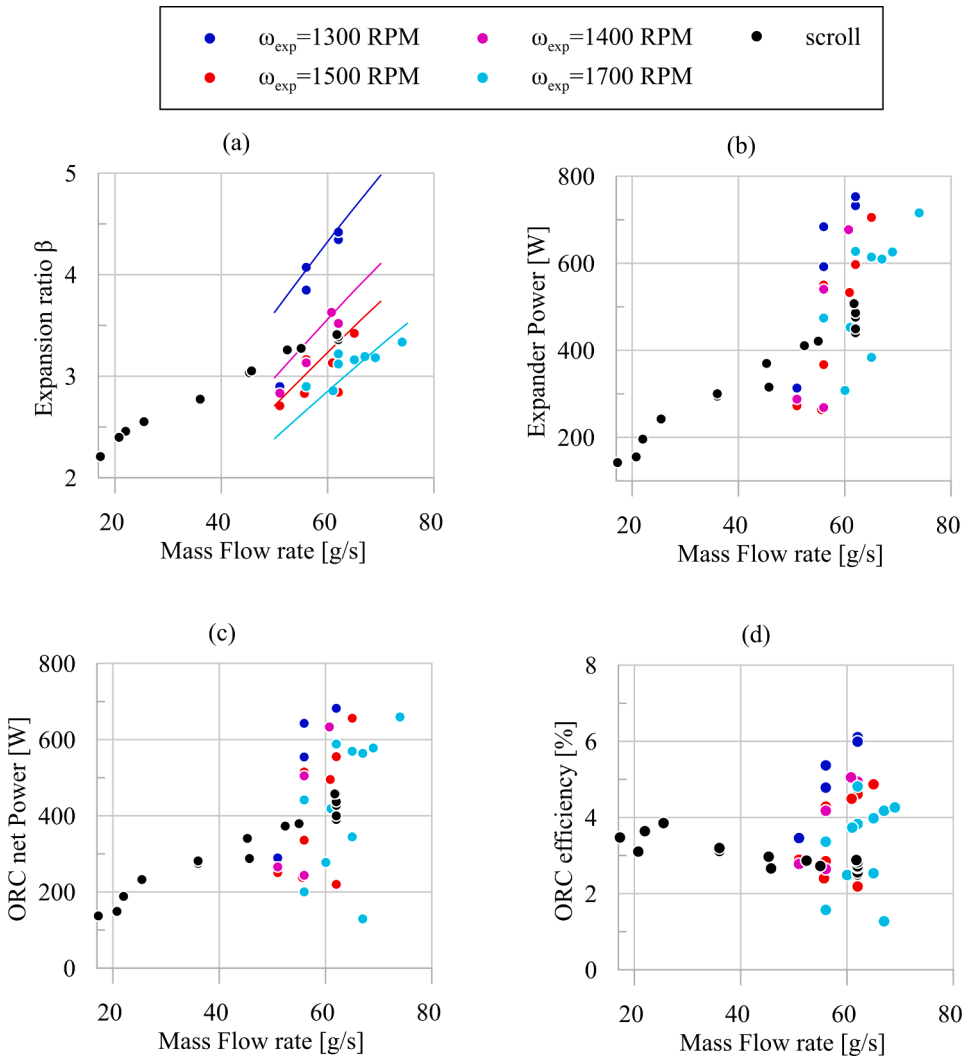

Fig. 14. Comparison between Scroll and SVRE in terms of expansion ratio (a) expander power (b) net ORC power (c) and efficiency (d).

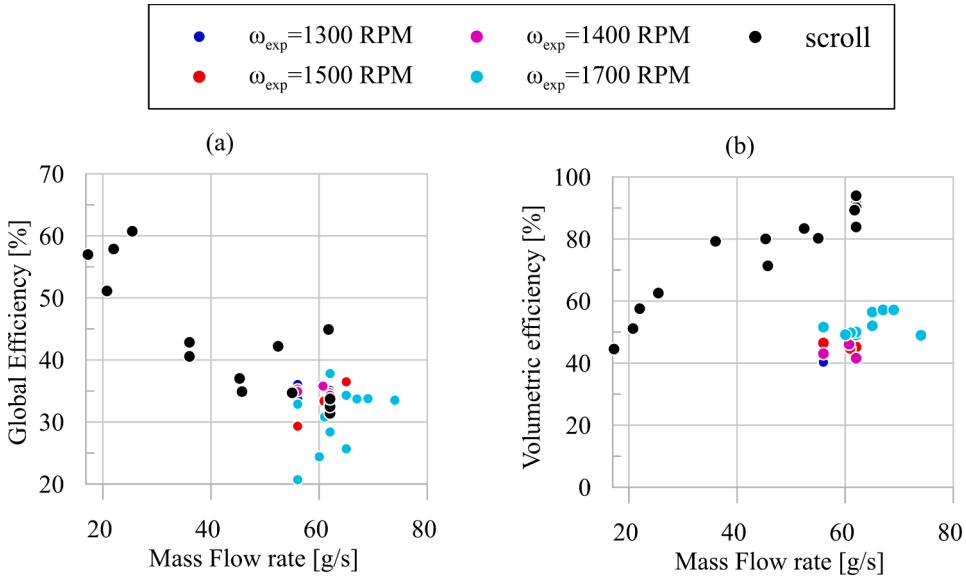

Fig. 15. Comparison between Scroll and SVRE volumetric (a) and global (b) efficiencies.

impact of power losses due to friction is larger in the Scroll case and depresses the net mechanical power (Fig. 14 (b)). These features reflect on the Net Power produced by the ORC unit (Fig. 14 (c)) which varies between 100–500 W and 200–700 W for Scroll and SVRE respectively. The Net Power values achieved when the SVRE was installed explains the higher efficiency of the unit in the 2 %-6% range (Fig. 14(d)) with respect to the Scroll configuration in the 2 %-4% range.

Based exclusively on the experimental evidence SVRE should be preferred to Scroll expander. Nevertheless the scroll machine is suitable for operation with low mass flow rate of working fluid: the volumetric efficiency increases from 40 % to 80 % when the mass flow rate increases between 17 g/s and 40 g/s (Fig. 15 (b)) proving that the mass flow rate that effectively enters the chambers is large enough to guarantee a suitable pressure difference across the expander despite the volumetric losses. The relative advantage with respect to the SVRE expander that does not start with less than 50 g/s mass flow rates appears evident. A further benefit of Scroll expanders is in the faster start-up phase with respect to the SVRE expander: whereas both SVRE and Scroll machines tolerate dual phase expansions SVRE only starts in presence of a superheated vapor i.e. only with a superheating degree above an assigned threshold. This means that whereas the Scroll machine could start as soon as the expansion ratio is sufficient to move the machine the SVRE begins to work only with a fully vaporized working fluid. Nevertheless during operation SVRE tolerates two-phases working fluid. The last comparison between the two machines was performed in terms of global efficiency. The SVRE presents a flatter global efficiency trend as a function of mass flow rate with an average 40 % value (Fig. 15 (a)); the Scroll expander instead shows a clear decrease of global efficiency when the mass flow rate grows. Main reason for this is that the global efficiency is expresses the trade-off between the volumetric and mechanical efficiency trends. When the mass flow rate increases the pressure rises and consequently the revolution speed grows as observed in Section 3.2. The revolution speed increase produces an enhancement of volumetric efficiency which plays a positive effect on global performance. Nevertheless the increase of revolution speed leads to larger mechanical losses due to dry and viscous friction effect. When the mass flow rate is comprised between 40 g/s and 60 g/s the revolution speed is comprised between 4000 RPM and 6000 RPM. Hence the mechanical losses play a dominant effect on the global efficiency in the 30 % − 40 % range. On the other hand for mass flow rates between 17 g/s and 40 g/s the global efficiency ranges between 60 % and 40 %. It is worth to remind that expander global efficiency (Eq. (2)) expresses the difference between the real machine behavior (shaft power) with the ideal one identified in literature as an adiabatic isentropic efficiency [31]. Hence the expander global efficiency takes into account the combined effects of volumetric fluid-dynamic and mechanical losses on the whole expander performance. Scroll expander shows an efficiency in line with literature results [29,31]. Also for SVRE the expander global efficiency complies with the literature results [30,32].

6. Conclusions

In the present paper an experimental and theoretical analysis of Micro-Cogenerative Solar ORC-based power unit is presented. The analysis accounts for two different unit configurations based on the expander type and regulation strategy: the plant features either a Scroll expander whose revolution speed varies with the operating conditions since the electrical generator is connected to a resistive load or a sliding vane rotary expander whose revolution speed is set regardless of the operating conditions via a dedicated inverter. The difference in the regulation strategy is due to the connection between expander and generator in the two cases. This aspect represents the only difference in plant set-up being the hydraulic connection the same in the two cases.

Despite the two considered machines present different volume size rated revolution speed and volumetric efficiency values they provide similar amount of elaborated flow rate for a given set of operating conditions. Again the performances of both plant configurations were experimentally assessed and compared. The results in terms of machine efficiency and power produced can be retained independent from the layout selected as this choice does not affect the kind and the amount of volumetric and mechanical losses which on turn are related to the expander technology. This aspect is demonstrated by the agreement of efficiency and power values with the one reported in literature for similar machine and the same working fluid (R245fa). For this reason the different layout was seen as an opportunity to assess the impact of regulation strategy on machine operability which is the main results of the control procedure. Basically it was compared the expander regulation imposing its revolution speed (SVRE case) and leaving this value free to varied according to the dynamic condition on the shaft (Scroll case). To support the analysis two validated models of the considered regulation approaches were developed based on the reproduction on machine permeability. Both models were experimentally validated and allowed to demonstrate that all the positive displacement expander behaves as a revolving valve whose permeability defines the relation between plant maximum pressure and mass flow rate. The regulation of revolution speed ensures to break the univocal relation between these quantities (SVRE case) typical of the case of uncontrolled expander speed.

Concerning the performance comparison between the two ORC plant configuration 200 W–700 W net power is produced in the SVRE set-up with a 2–6 % efficiency. Such values exceed the corresponding ones for the Scroll set-up (100 W–500 W net power and 2–4 % efficiency) largely due to larger frictional losses associated with the higher revolution speed of the Scroll machine. Such an effect becomes particularly relevant at higher mass flow rates for which the global efficiency of the Scroll expander tops 30–40 % in spite of a volumetric efficiency in the 80–90 % range. On the contrary scroll machine presents a shorter starting time and allows to operate in a wider operating range. This makes the expander selection not straightforward and intimately related to the expected operating condition. In any case global expander efficiencies between 30 % and 40 % represents a severe limiting factor for a net power in the range of 200 W–700 W when flow rate are in a range between 50 and 80 g/s. It is worth to notice that SVRE benefits from revolution speed management which ensure to vary the intake pressure to maximize the performance. This layout should be preferred independently from the used machine. Indeed it allows to control the revolution speed.

Despite such aspect SVRE presents lower efficiency than scroll machine which cannot exploit the advantage of revolution speed control. Considering all the collected results of these two set-ups SVRE might be the best option due to the higher ORC power and efficiency. On the other hand scroll machine present a higher machine efficiency a wider operability range and a lower start time. Indeed scroll expander can work even if the working fluid is not fully vaporized yet thus it runs quite immediately after the starting of the pump. Conversely SVRE tolerates dual phase expansion during operation but only starts once the working fluid is completely vaporized i.e. few minutes after the pump is started.

CRediT authorship contribution statement

Fabio Fatigati: Conceptualization, Methodology, Software, Validation, Data curation, Investigation, Writing – original draft, Visualization, Writing – review & editing. **Diego Vittorini:** Conceptualization, Methodology, Investigation, Writing – original draft, Visualization, Writing – review & editing. **Arianna Coletta:** Data curation, Investigation, Writing – original draft. **Roberto Cipollone:** Conceptualization, Methodology, Supervision, Investigation, Writing – original draft, Visualization, Project administration, Writing – review & editing.

Declaration of Competing Interest

The authors declare that they have no known competing financial

interests or personal relationships that could have appeared to influence the work reported in this paper.

Data availability

Data will be made available on request.

Acknowledgments

The authors are deeply grateful to SIVAM s.r.l in particular to its C.E.O. Paolo Orsini for the support given during this activity. The authors would like to acknowledge also Sanden S.p.A. and Ing. Enea Mattei S.p.A for the technical support given during the present research.

References

[1] Cioccolanti L, Tascioni R, Bocci E, Villarini M. Parametric analysis of a solar Organic Rankine Cycle trigeneration system for residential applications. Energy Convers Manage 2018;163:407–19.
[2] Polanco Piñerez G, Valencia Ochoa G, Duarte-Forero J. Energy, exergy, and environmental assessment of a small-scale solar organic Rankine cycle using different organic fluids. Heliyon 2021;7(9):e07947.
[3] Aboelwafa O, Fateen SK, Soliman A, Ismail IM. A review on solar Rankine cycles: Working fluids applications and cycle modifications Renew. Sustain Energy Rev 2018;82:868–85. https://doi.org/10.1016/j.rser.2017.09.097. ISSN 1879-0690.
[4] Eterafi S, Gorjian S, Amidpour M. Thermodynamic design and parametric performance assessment of a novel cogeneration solar organic Rankine cycle system with stable output. Energy Convers Manage 2021;243:114333.
[5] Loni R, Mahian O, Markides CN, Bellos E, le Roux WG, Kasaeian A, et al. A review of solar-driven organic Rankine cycles: Recent challenges and future outlook. Renew Sustain Energy Rev 2021;150:111410.
[6] Garcia-Saez I, Mendez J, Ortiz C, Loncar D, Becerra JA, Chacartegui R. Energy and economic assessment of solar Organic Rankine Cycle for combined heat and power generation in residential applications. Renew Energy 2019;140:461–76. https://doi.org/10.1016/j.renene.2019.03.033. ISSN 0960-1481.
[7] Pereira JS, Ribeiro JB, Mendes R, Vaz GC, André JC. ORC based micro-cogeneration systems for residential application – A state of the art review and current challenges. Renew Sustain Energy Rev 2018;92:728–43. https://doi.org/10.1016/j.rser.2018.04.039. ISSN 1879-0690.
[8] Pina EA, Lozano MA, Serra LM, Hernández A, Lázaro A. Design and thermoeconomic analysis of a solar parabolic trough – ORC – Biomass cooling plant for a commercial center. Sol Energy 2021;215:92–107.
[9] Gupta PR, Tiwari AK, Said Z. Solar organic Rankine cycle and its poly-generation applications –A review. Sustain Energy Technol Assess 2022;49:1–5. https://doi.org/10.1016/j.seta.2021.101732. ISSN 2213-1388.
[10] Aghaziarati Z, Aghdam AH. Thermoeconomic analysis of a novel combined cooling heating and power system based on solar organic Rankine cycle and cascade refrigeration cycle. Renew Energy 2021;164:1267–83. https://doi.org/10.1016/j.renene.2020.10.106. ISSN 0960-1481.
[11] Xi Z, Eshaghi S, Sardari F. Energy, exergy, and exergoeconomic analysis of a polygeneration system driven by solar energy with a thermal energy storage tank for power, heating, and freshwater production. J Energy Storage 2021;36:102429. https://doi.org/10.1016/j.est.2021.102429.
[12] Mosaffa AH, Garousi L. Farshi Thermodynamic and economic assessments of a novel CCHP cycle utilizing low-temperature heat sources for domestic applications. Renew Energy 2018;120:134–50. https://doi.org/10.1016/j.renene.2017.12.099. ISSN 0960-1481.
[13] Eisavi B, Nami H, Yari M, Ranjbar F. Solar-driven mechanical vapor compression desalination equipped with organic Rankine cycle to supply domestic distilled water and power – Thermodynamic and exergoeconomic implications. Appl Therm Eng 2021;193:116997. https://doi.org/10.1016/j.applthermaleng.2021.116997. ISSN 1359-4311.
[14] IEA (IEA (International Energy Agency) Tracking Buildings 2020 – Analysis www.iea.org/reports/tracking-buildings-2020.
[15] Pang K-C, Hung T-C, He Y-L, Feng Y-Q, Lin C-H, Wong K-W. Developing ORC engineering simulator (ORCES) to investigate the working fluid mass flow rate control strategy and simulate long-time operation. Energy Convers Manage 2020;203:112206.
[16] Marinheiro MM, Coraça GM, Cabezas-Gómez L, Ribatski G. Detailed transient assessment of a small-scale concentrated solar power plant based on the organic Rankine cycle. Appl Therml Eng 2022;204:117959. https://doi.org/10.1016/j.applthermaleng.2021.117959. ISSN 1359-4311.
[17] Hu B, Guo J, Yang Yu, Shao Y. Solar powered organic Rankine-vapor compression air conditioning. Energy Reports 2022;8:207–13.
[18] Yu H, Helland H, Yu X, Gundersen T, Sin G. Optimal design and operation of an Organic Rankine Cycle (ORC) system driven by solar energy with sensible thermal energy storage. Energy Convers Manage 2021;244:114494.
[19] Sun K, Zhao T, Wu S, Yang S. Comprehensive evaluation of concentrated solar collector and Organic Rankine cycle hybrid energy process with considering the effects of different heat transfer fluids. Energy Reports 2021;7:362–84.
[20] Zhou F, Ji J, Yuan W, Zhao X, Huang S. Study on the PCM flat-plate solar collector system with antifreeze characteristics. Int J Heat Mass Transf 2019;129:357–66. https://doi.org/10.1016/j.ijheatmasstransfer.2018.09.114. ISSN 1879-2189.
[21] Lizana J, Bordin C, Rajabloo T. Integration of solar latent heat storage towards optimal small-scale combined heat and power generation by Organic Rankine Cycle. J Energy Storage 2020;29:101367.
[22] Vittorini D, Antonini A, Cipollone R, Carapellucci R, Villante C. Solar Thermal-Based ORC Power Plant for Micro Cogeneration – Performance Analysis and Control Strategy. Energy Procedia 2018;148:774–81.
[23] Pantano F, Capata R. Expander selection for an on board ORC energy recovery system. Energy 2017;141:1084–96.
[24] Fatigati F, Di Battista D, Cipollone R. Cipollone Permeability effects assessment on recovery performances of small-scale ORC plant. Appl Therm Energy 2021;196:117331.
[25] Guo Z, Zhang C, Wu Y, Lei B, Yan D, Zhi R, et al. Numerical optimization of intake and exhaust structure and experimental verification on single-screw expander for small-scale ORC applications. Energy 2020;199:117478.
[26] Fatigati F, Vittorini D, Di Bartolomeo M, Cipollone R. Experimental characterization of a small-scale solar Organic Rankine Cycle (ORC) based unit for domestic microcogeneration. Energy Convers Manage 2022;258:115493.
[27] Moradi R, Villarini M, Cioccolanti L. Experimental modeling of a lubricated, open drive scroll expander for micro-scale organic Rankine cycle systems. Appl Therm Eng 2021;190:116784.
[28] Oh J, Jeong H, Kim J, Lee H. Numerical and experimental investigation on thermal-hydraulic characteristics of a scroll expander for organic Rankine cycle. Appl Energy 2020;278:115672.
[29] Ziviani D, James NA, Accorsi FA, Braun JE, Groll EA. Experimental and numerical analyses of a 5 kWe oil-free open-drive scroll expander for small-scale organic Rankine cycle (ORC) applications. Appl Energy 2018;230:1140–56.
[30] Mascuch J, Novotny V, Vodicka V, Spale J, Zeleny Z. Experimental development of a kilowatt-scale biomass fired micro – CHP unit based on ORC with rotary vane expander. Renew Energy 2020;147:2882–95.
[31] Declaye S, Quoilin S, Guillaume L, Lemort V. Experimental study on an open-drive scroll expander integrated into an ORC (Organic Rankine Cycle) system with R245fa as working fluid. Energy 2013;55:173–83.
[32] Naseri A, Moradi R, Norris S, Subiantoro A. Experimental investigation of a revolving vane expander in a micro-scale organic Rankine cycle system for low-grade waste heat recovery. Energy 2022;253:124174.